Design Investigation of an *X*-Band SIW H-Plane Band Pass Filter with Improved Stop Band Using Neural Network Optimization

Zahra S. Tabatabaeian and Mohammad H. Neshati

Department of Electrical Engineering
Ferdowsi University of Mashhad, 91779-48974, Mashhad, Iran
ztaba14@gmail.com, neshat@um.ac.ir

Abstract ─ In this paper, an *X*-band H-plane band pass filter based on substrate integrated waveguide (SIW) technology is introduced. Back propagation neural network (BPNN) method is applied to optimize parameters of the proposed filter. The stop band of the proposed filter is improved by cascading the H-plane filter with a low pass filter designed and implemented using defected ground structure (DGS). A prototype of the proposed filter is made and experimental results are presented and also compared with those obtained by simulation. Measured reflection coefficient and transmission coefficient in pass band are better than -20 dB and -3.7 dB respectively. Measured results agree well with those obtained by simulation.

Index Terms – Band pass filter, neural network, Substrate Integrated Waveguide (SIW).

I. INTRODUCTION

Microwave filters using rectangular metallic waveguides have been widely used in microwave communication systems. In recent years, a new kind of microwave transmission structure named substrate integrated waveguide (SIW) [1] has been introduced. SIW structures have similar propagation characteristics as the conventional metallic rectangular waveguide. They offer all advantages of rectangular waveguide and planar structures such as low insertion loss, high quality factor and easily integration with planar structures [1]. Moreover, they are low profile and their fabrication cost is low, especially in a production line. Based on the SIW technology, many passive and active devices such as filters, couplers [2], antennas [3] and mixers [4] have been proposed and successfully realized and tested.

Simulation process for SIW structure often requires a relative long time due to existence of via arrays, which needs to be meshed, leading to increasing the complexity of calculation. In turn, an optimization procedure is required to improve design and implementation of microwave components.

In this paper, a microwave H-plane filter is designed, optimized and numerically investigated. Using back propagation neural network (BPNN) method, an optimization process is applied to obtain filter parameters. To improve stop band response of the filter, a low pass filter using defected ground structure (DGS) is added to the proposed filter. The designed filter is numerically studied using high frequency structure simulator (HFSS).

II. THE H-PLANE FILTER DESIGN

The top view of the proposed filter and its geometrical parameters are shown in Fig. 1. It consists of seven cascaded rectangular cavities. The via holes have a diameter of d and the distance between two adjacent vias is denoted by S. The proposed filter is symmetric along AA' line in such a way that $W_i=W_{n+1-i}$ and $l_i=l_{n-i}$. TLY031 is used as the substrate with ε_r=2.2 and h=0.787 mm. The desired pass band is considered between f_1=9.5 GHz and f_2=10.5 GHz.

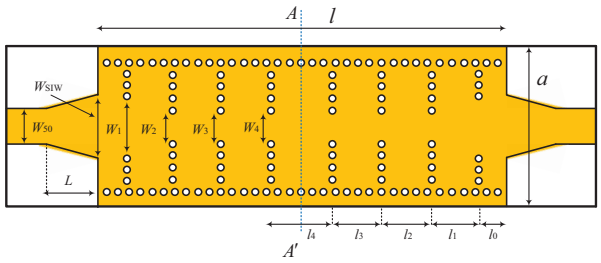

Fig. 1. The proposed H-plane filter structure.

At first, the parameters of the proposed filter are designed based on conventional rectangular waveguide formula, and then, they are adjusted for SIW structures using equivalent width formula. The fractional bandwidth of the proposed filter is defined by Equation (1) [5]:

$$FB_{\lambda} = \frac{\lambda_{g1} - \lambda_{g2}}{\lambda_{go}}, \quad (1)$$

in which

$$\lambda_{go} = \frac{\lambda_{g1} + \lambda_{g2}}{2}, \quad (2)$$

Submitted On: October 31, 2014
Accepted On: August 14, 2015

$$\lambda_{gi} = \frac{c}{f_i\sqrt{1-\left(f_c/f_i\right)^2}}\frac{1}{\sqrt{\varepsilon_r}} \quad i=1,2, \tag{3}$$

$$f_c = \frac{c}{2a_{RW}}, \tag{4}$$

c and a_{RW} are light velocity in free space and the equivalent rectangular waveguide width respectively. Then, from the following equations, impedance invert values of the conventional rectangular waveguide is evaluated [5]:

$$\frac{K_{o1}}{Z_o} = \sqrt{\frac{\pi FB_\lambda}{2g_o g_1}}, \tag{5}$$

$$\frac{K_{i,i+1}}{Z_o} = \frac{\pi FB_\lambda}{2}\sqrt{\frac{1}{g_i g_{i+1}}} \quad i=1,2,....,n-1, \tag{6}$$

$$\frac{K_{n,n+1}}{Z_o} = \sqrt{\frac{\pi FB_\lambda}{2g_n g_{n+1}}}, \tag{7}$$

where g_0, g_1, g_2, …, g_{n+1} are normalized elements of seventh order Chebyshev with 0.01 dB ripple. The susceptance values of symmetrical windows can be enhanced as follows:

$$\frac{X_{i,i+1}}{Z_o} = \frac{K_{i,i+1}/z_o}{1-\left(K_{i,i+1}/z_o\right)^2}. \tag{8}$$

In return, width W_{RWi} (i=1, 2, …, n+1) of symmetrical window can be obtained by Equations (9) and (10) [5]:

$$\frac{X}{Z_o} = \frac{a_{RW}}{\lambda_{go}}\tan^2\left\{\frac{\pi W_{RWi}}{2a_{RW}}\left[1+\frac{1}{6}\left(\frac{\pi W_{RWi}}{\lambda_o}\right)^2\right]\right\}, \quad \frac{W_{RWi}}{a_{RW}} \ll 1, \tag{9}$$

$$\frac{X}{Z_o} = \frac{a_{RW}}{\lambda_{go}}\cot^2\left\{\frac{\pi W'_{RWi}}{2a_{RW}}\left[1+\frac{2}{3}\left(\frac{\pi W'_{RWi}}{\lambda_o}\right)^2\right]\right\}, \quad \frac{W'_{RWi}}{a_{RW}} \gg 1, \tag{10}$$

in which

$$W'_{RWi} = \frac{a_{RW}-W_{RWi}}{2}, \tag{11}$$

$$\lambda_o = \frac{c}{\sqrt{f_1 f_2}}. \tag{12}$$

Finally, l_{iRW} can be obtained using Equation (13) [5]:

$$l_{RWi} = \frac{\lambda_{go}}{2\pi}\theta_i, \tag{13}$$

$$\theta_i = \pi - \frac{1}{2}\left[\tan^{-1}\left(\frac{2X_{i-1,i}}{Z_o}\right)+\tan^{-1}\left(\frac{2X_{i,i+1}}{Z_o}\right)\right]. \tag{14}$$

The parameters W_i, l_i and a of SIW structure can be obtained from W_{RWi}, l_{RWi} and a_{RW}, using the following equation [6]:

$$W_{RW} = \frac{W_{SIW}}{\sqrt{1+\left(\frac{2W_{SIW}-d}{S}\right)\left(\frac{d}{W_{SIW}-d}\right)^2-\frac{4W_{SIW}}{5S^4}\left(\frac{d^2}{W_{SIW}-d}\right)^3}}.$$

III. NEURAL NETWOK OPTIMIZATION

Back propagation neural network (BPNN) is generally used in function approximation. In fact, BPNN is a non-linearity artificial neural network and it has been proved that any continuous function in enclosed interval can be approached by a BPNN with a hidden layer. A BPNN model is shown in Fig. 2.

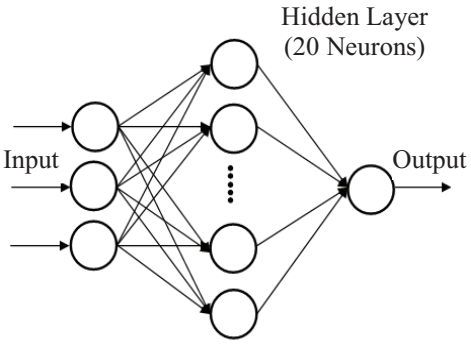

Fig. 2. Back propagation neural network model.

A. Back propagation algorithm

A back propagation (BP) network has to be trained. Input vectors and the corresponding target vectors are used to train a network until it could approximate the required function. BPNN use a gradient descent algorithm, in which the network weights are moved along the negative of the gradient of the performance function. Properly trained back propagation networks tend to give reasonable answers when presented with inputs that they have never seen.

B. Levenberg-Marquardt back propagation

The trainlm training function is chosen to train the network in this paper. It is a network training function that updates weight and bias values according to Levenberg-Marquardt optimization. Trainlm is often the fastest back propagation algorithm in the toolbox, and is highly recommended as a first choice supervised algorithm; although, it does require more memory than the other algorithms [7].

IV. OPTIMIZATION PROCEDURE

The basic parameters of the filter are shown in Fig. 1. W_{SIW} is chosen from 5 mm to 9 mm, L is varied from 6 mm to 12 mm and W_{50} is selected from 1.854 mm to 2.854 mm. W_{SIW}, L and W_{50} are chosen to be the input of the neural network and the maximum of S_{11} in the pass band is considered to be the output of the optimization process. The neural network has 20 neurons in its hidden layer and the training function is chosen trainlm. Table 1 summarizes few training data and their reported S_{11} which are obtained using HFSS. Testing data are summarized in Table 2. The testing data show that the

BPNN output data and S_{11} results obtained from HFSS agree well with each other.

After training the neural network, the optimum values of the inputs in which maximum S_{11} in the pass band is minima can be derived. The values for different parameters of the proposed filter are listed in Table 3 and optimum parameters W_{SIW}, L and W_{50} are 7.07 mm, 7.80 mm and 2.65 mm, respectively.

Table 1: Training data for the optimization procedure

W_{SIW} (mm)	L (mm)	W_{50} (mm)	S_{11} (dB)
5	10	2.354	-8.81
7	12	2.354	-10.46
9	8	2.354	-11.20
7	8	2.604	-22.10
7	10	2.104	-15.63
7	8	2.104	-14.39
9	10	2.104	-14.64
7	8	2.854	-17.65

Table 2: Testing data for the optimization procedure

W_{SIW} (mm)	L (mm)	W_{50} (mm)	S_{11} (dB) (BPNN)	S_{11} (dB) (HFSS)
8.1	7.5	2.8	-20.01	-19.83
5.2	7.6	2.4	-12.73	-12.84
6.4	8.6	2.6	-19.58	-19.28
7.8	11.2	2	-12.70	-13.03
7.3	7.1	2.5	-18.22	-18.38
7.5	7.9	1.9	-10.64	-10.47
7.6	9	2.3	-16.13	-16.15

Table 3: The geometrical parameters of the proposed filter

Parameter	Value (mm)	Parameter	Value (mm)
a	20.67	l_0	8.03
l	90.0	l_1	9.54
d	1.0	l_2	10.79
W_1	10.48	l_3	11.08
W_2	7.66	l_4	11.12
W_3	6.86	h	0.787
W_4	6.7	S	1.5

V. RESULTS AND DISCUSSIONS

Simulated S-parameters of the designed filter using the optimized parameters versus frequency are shown in Fig. 3 (a) and Fig. 3 (b). The optimum value of S_{11} is -24.90 dB, which agrees well with the result obtained using HFSS which is -24.37 dB. It can be seen that the stop band of the filter is very small; especially the second harmonic of the input is suppressed only -3 dB. In order to improve the stop band characteristic of the proposed filter, two low pass filters are cascaded, one at the input port and the other at the output.

A. Low pass DGS filter

A defected ground structure (DGS) low pass filter is chosen to improve the stop band response of the proposed filter. Figure 4 shows the DGS structure of the filter. In this structure g=0.3 mm, v_2=1.2 mm, v_1=0.7 mm and l_i can be obtained by means of Equations (15) and (16) [8]. Distance between different defect parts is uniform and designated by l:

$$l_i = \frac{N_3}{N_i} l_3 \quad i = 1,2,3, \tag{15}$$

$$N_i = \sqrt[i]{C}. \tag{16}$$

C is constant. By increasing C, return loss in pass band will be increased [8]. In this paper, C and l_3 are chosen 3.3 and 2.2 mm, respectively. So, l_1=1 mm and l_2=1.8 mm are calculated. Geometrical parameters of the DGS filter are summarized in Table 4.

B. Simulation results of the DGS filter

Simulated S-parameters of the designed DGS filter are shown in Fig. 5. It can be seen that maximum insertion loss in pass band is 3.48 dB, while between 16 GHz to 20 GHz stop band attenuation is at least 40 dB.

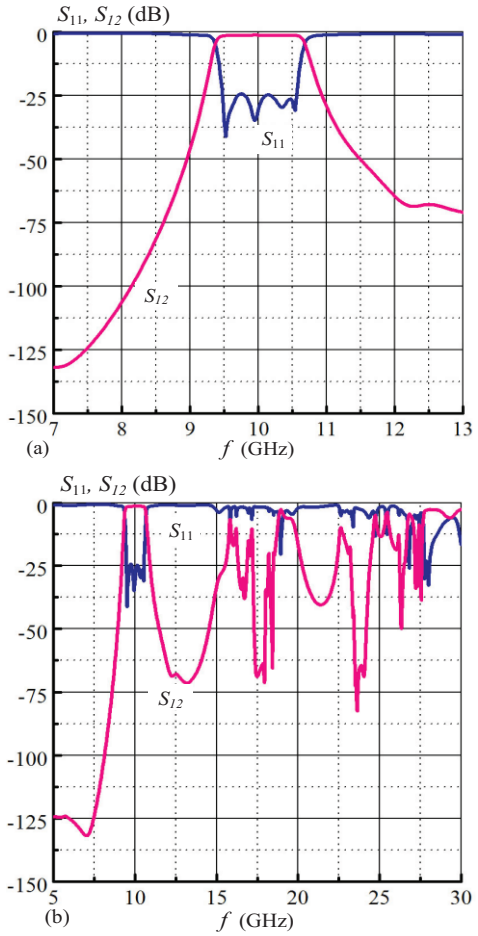

Fig. 3. Simulated S-parameters of the proposed filter using optimized parameters for two frequency ranges: (a) narrowband and (b) wideband.

Table 4: Geometrical parameters of the DGS structure

Parameter	Value (mm)
l_1	1
l_2	1.8
l_3	2.2
v_1	0.7
v_2	1.2
g	0.3
l	1.2

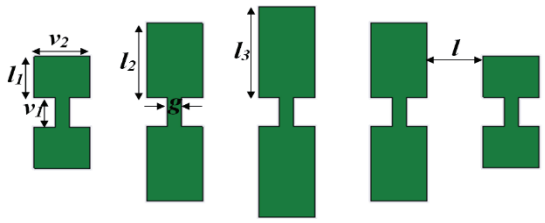

Fig. 4. DGS structure for the proposed filter.

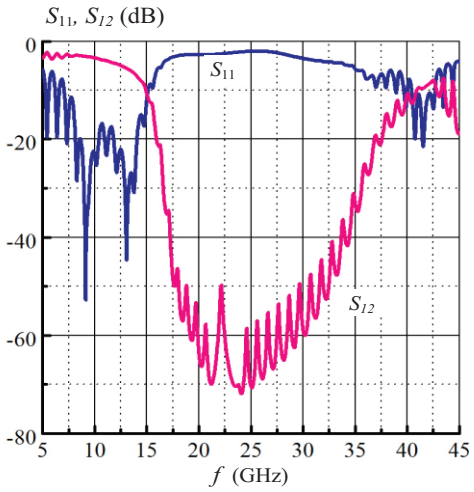

Fig. 5. Simulated *S*-parameters of the proposed DGS structure.

C. Simulation results of the filter with DGS

The designed filters are cascaded with each other. The final filter structure and its simulated frequency response are shown in Fig. 6 and Fig. 7 respectively. It can be seen that the applied DGS low pass filter suppress the undesired harmonics and the stop band of the filter response is highly improved. It can be seen that a very wide stop band bandwidth, with at least 20 dB attenuation is obtained by the proposed filter. However, passband insertion loss is increased by a little compared to that of the filter without DGS. The obtained results show that simulated S_{11} and insertion loss are better than -23 dB and 3 dB in pass band respectively, while stop band attenuation is at least 20 dB. The simulated detailed performance of the proposed filter with optimized parameters including DGS filter are listed in Table 5. Also, simulated characteristics of a few recently published research are also summarized in this table for comparison.

D. Measured results

To evaluate the designed procedure of the proposed filter, a prototype of the proposed filter is fabricated using TLY031 substrate with electrical characteristics including: ε_r=2.2, h=0.787 mm and tan loss of 0.009. The photo of the fabricated filter is shown in Fig. 8. *S*-parameters of the filter are measured using HP 8510 network analyzer. The measured results are shown in Figs. 9 (a) and 9 (b), including the simulation results for comparison. It can be seen that the obtained S_{11} is better than -20 dB in pass band. Also, insertion loss of the filter is better than 3.7 dB in pass band and the attenuations of the filter is better than 19 dB in stop band. Moreover, a very good agreement is obtained between measured and simulated results.

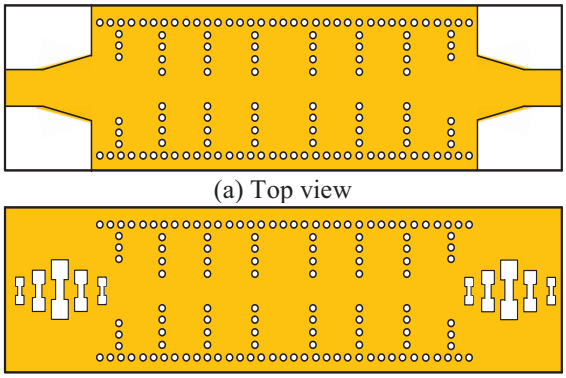

Fig. 6. Structure of the proposed filter with DGS.

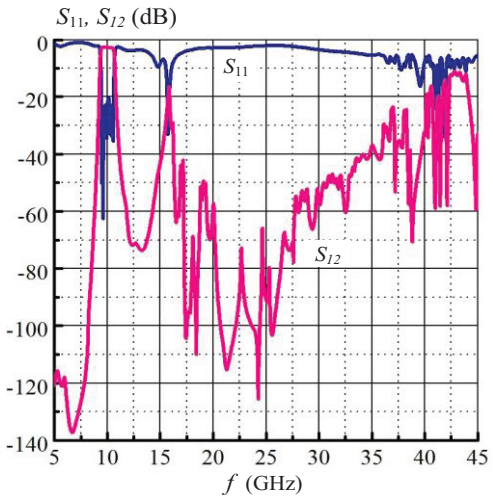

Fig. 7. Simulated *S*-parameters of the proposed filter with DGS.

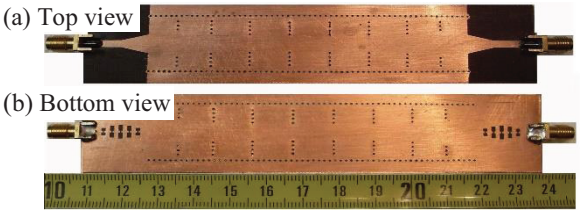

Fig. 8. The photo of the fabricated filter.

Table 5: Comparison of the simulated performance of the proposed filter with recently published ones

Filter	*FBW* (%)	S_{11} (dB)	S_{21} (dB)	End of the Stopband (GHz)
[9]	5.8	<-22	-1.7	16.7
[10]	7.6	<-14	-1.3	14
[11]	8	<-27	-2	25
[12]	5	<-12.5	-4.3	20.2
[13]	18.7	<-20	-2.3	12.2
[14]	4	<-10	-3.8	12.6
[15]	4.9	<-8	-1	18.2
[16]	4.9	<-17.6	-2.6	13.8
This paper	13	<-23.6	-3	40.6

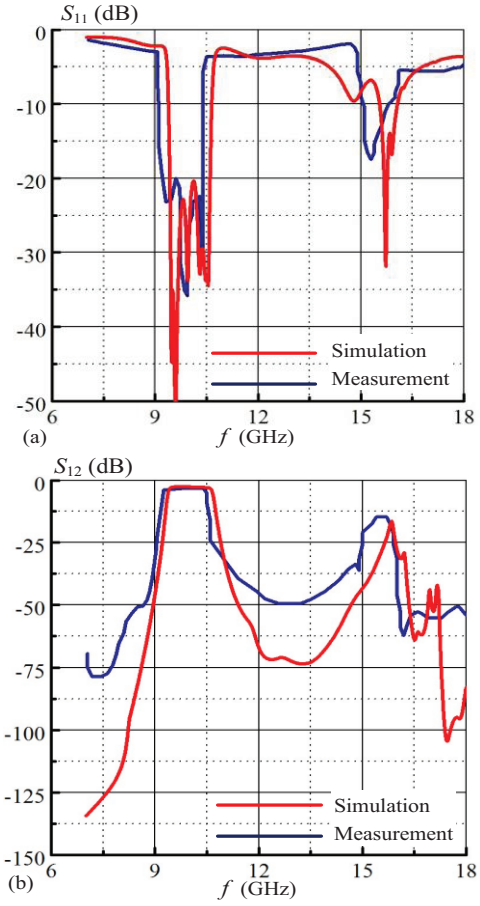

Fig. 9. Simulation and measurement results of the fabricated filter: (a) S_{11}, and (b) S_{12} in a narrowband region.

VI. CONCLUSION

An *X*-band H-plane filter cascaded with a DGS structure is designed based on neural network and numerically investigated using HFSS in this paper. Back propagation neural network is applied to optimize the parameters of the proposed filter. Results show that, measured reflection coefficient and transmission coefficient are -20 dB and -3.7 dB respectively. In addition, a very good agreement is obtained between measured results and those obtained by simulation. Moreover, it is concluded that neural network is very useful for optimizing microwave devices.

REFERENCES

[1] D. Deslandes and K. Wu, "Integrated microstrip and rectangular waveguide in planar form," *IEEE Microw. Wireless Compon. Lett*., vol. 11, no. 2, pp. 68-70, Feb. 2001.

[2] D. F. Guan, Z. P. Qian, Y. S. Zhang, and Y. Cai, "A hybrid SIW and GCPW guided-wave structure coupler," *IEEE Microw. Wireless Compon. Lett*., vol. 24, iss. 8, pp. 518-520, 2014.

[3] H. Dashti, M. Shahabadi, and M. H. Neshati, "SIW cavity-backed slot antennas with improved gain," *21st Iranian Conference on Electrical Engineering*, pp. 1-4, 2013.

[4] F. F. He, K. Wu, W. Hong, L. Han, and X. P. Chen, "Low-cost 60-GHz smart antenna receiver subsystem based on substrate integrated waveguide technology," *IEEE Transactions on Microwave Theory and Techniques*, vol. 60, iss. 4, pp. 1156-1165, 2012.

[5] X. Zou, C. Tong, and D. Yu, "Design of an X-band symmetrical window bandpass filter based on substrate integrated waveguide," *Cross Strait Quad-Regional Radio Science and Wireless Technology Conference*, pp. 571-574, 2011.

[6] M. Salehi and E. Mehrshahi, "A closed-form formula for dispersion characteristics of fundamental SIW mode," *IEEE Microwave and Wireless Components Letters*, vol. 21, pp. 4-6, 2011.

[7] *Fecit R&D Center of Science and Technology Products, Neural Network Theory and Matlab Implementation*, Beijing: Publishing House of Electronics Industry, 2005.

[8] P. Vagner and M. Kasal, "Design of microstrip lowpass filter using DGS," *Radio Elektronika, 17th International Conference*, pp. 1-4, 2007.

[9] J. D. Martinez, S. Sirci, M. Taroncher, and V. E. Boria, "Compact CPW-fed combline filter in substrate integrated waveguide technology," *IEEE Microwave and Wireless Components Letters*, vol. 22, pp. 7-9, 2012.

[10] L. S. Wu, Y. X. Guo, J. F. Mao, and W. Y. Yin, "Design of a substrate integrated waveguide balun filter based on three-port coupled-resonator circuit

model," *IEEE Microwave and Wireless Components Letters*, vol. 21, pp. 252-254, 2011.

[11] Y. Fei, L. Rui-zhu, and Y. Hong-xi, "Canonical ridged SIW filters in LTCC," *IEEE International Conference on Microwave Technology & Computational Electromagnetics*, pp. 190-192, 2011.

[12] G. S. Huang and C. H. Chen, "Non uniformly folded waveguide resonators and their filter applications," *IEEE Microwave and Wireless Components Letters*, vol. 20, pp. 136-138, 2010.

[13] P. Hong and H. Jin, "Half mode substrate integrated waveguide bandpass filter using cross-coupling," *International Conference on Computational Problem-Solving*, pp. 196-198, 2012.

[14] F. T. Ladani, S. Jam, and R. Safian, "A novel X-band bandpass filter using substrate integrated waveguide resonators," *IEEE Asia-Pacific Conference on Applied Electromagnetics*, pp. 1-5, 2010.

[15] E. Mehrshahi, M. Salehi, and R. Rezaiesarlak, "Substrate integrated waveguide filters with stopband performance improvement," *International Conference on Microwave and Millimeter Wave Technology*, pp. 2018-2020, 2010.

[16] L. S. Wu, X. L. Zhou, and W. Y. Yin, "A novel multilayer partial H-plane filter implemented with folded substrate integrated waveguide," *IEEE Microwave and Wireless Components Letters*, vol. 19, pp. 494-496, 2009.

Zahra Sadat Tabatabaeian was born in Mashhad, Iran on May 7, 1988. She received her B.Sc. and M.Sc. degrees in Electrical Engineering from Ferdowsi University of Mashhad, Iran in 2010 and 2012 respectively, and now she is currently working toward her Ph.D. degree in Electrical Engineering at Ferdowsi University of Mashhad. Her research interests include microwave passive circuit design and meta-materials.

Mohammad H. Neshati was born in Yazd, Iran. He received his B.Sc. in Electrical Engineering from Isfahan University of Technology, Isfahan, Iran; M.Sc. degree from Amir-Kabir University of Technology, Tehran, Iran and Ph.D. from the University of Manchester (UMIST), England in 2000. Since 2006 he has been with the Department of Electrical Engineering of Ferdowsi University of Mashhad Iran, where he is Associate Professor. His current research includes electromagnetic, antenna theory and design, microwave active and passive circuit design.